Wireless Channel Modelling for Identifying Six Types of Respiratory Patterns with SDR Sensing and Deep Multilayer Perceptron

Umer Saeed, Syed Yaseen Shah, Adnan Zahid, Jawad Ahmad, *Senior Member, IEEE*, Muhammad Ali Imran, *Senior Member, IEEE*, Qammer H. Abbasi, *Senior Member, IEEE*, Syed Aziz Shah

***Abstract*— Contactless or non-invasive technology has a significant impact on healthcare applications such as the prediction of COVID-19 symptoms. Non-invasive methods are essential especially during the COVID-19 pandemic as they minimise the burden on healthcare personnel. One notable symptom of COVID-19 infection is a rapid respiratory rate, which requires constant real-time monitoring of respiratory patterns. In this paper, Software Defined Radio (SDR) based Radio-Frequency sensing technique and supervised machine learning algorithm is employed to provide a platform for detecting and monitoring various respiratory: eupnea, biot, bradypnea, sighing, tachypnea, and kussmaul. The variations in Channel State Information (CSI) produced by human respiratory were utilised to identify distinct respiratory patterns using fine-grained OFDM signals. The proposed platform based on the SDR and the Deep Multilayer Perceptron (DMLP) classifier exhibits the ability to effectively detect and classify the aforementioned distinct respiratory with an accuracy of up to 99%. Moreover, the effectiveness of the proposed scheme in terms of diagnosis accuracy, precision, recall, F1-score, and confusion matrix is demonstrated by comparison with a state-of-the-art machine learning classifier: Random Forest.**

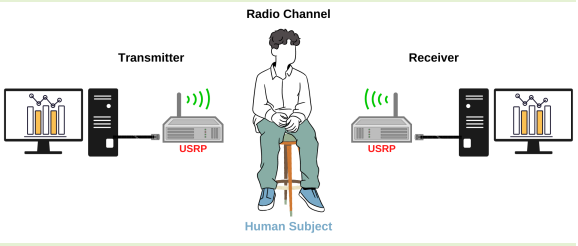

***Index Terms*— COVID-19, Abnormal Respiratory, Non-invasive, USRP, CSI, Software Defined Radio, Neural Network**

I. Introduction

COVID-19 or COrona VIrus Disease'19 has infected millions of people globally, and with the recent emergence of new variants in distinct parts of the world, the vaccine's effectiveness is at utmost concern. COVID-19 has been linked to more than 3 million deaths, according to the recent figure by World Health Organization (WHO) - `https://covid19.who.int`. Fever, flu, ageusia, cough, and lungs failure due to respiratory disorders are the most common symptoms of the virus, which spreads primarily by human-to-human contact. Governments all over the world are seeking to stop the epidemic from spreading by imposing frequent lockdowns, which is wreaking havoc on the economy and private businesses [1].

The novel variants of COVID-19 are directly targeting human lungs, consequently resulting severe damage towards the respiration. The average human respiratory rate for an adult at rest is between 12 and 20 breaths per minute, and it is irregular if it is less than 12 breaths per minute or more than 20 breaths per minute [2]. Respiratory rate that are abnormal may be sluggish, shallow, rapid, intense, or a hybrid of these. Figure 1 depicts the six diverse human respiratory or breathing patterns: eupnea, biot, bradypnea, sighing, tachypnea, and kussmaul. Eupnea is a regular respiratory with a normal rhythm and frequency caused by a healthy lifestyle, while biot is an intense respiratory with slow intervals of no breaths engendering by spinal meningitis or concussion (head injury). Bradypnea is a sluggish and shallow respiratory resulting from concussion, sleeping pills, stroke, or metabolic disorder. Sighing is respiratory stressed by recurrent intense breaths due to dyspnea, dizziness, or nervousness. Tachypnea is the opposite of bradypnea described as rapid and shallow respiratory as a result of anxiety, fever, stun, or exercise. Lastly, kussmaul is an intense and rapid respiratory pattern by virtue of diabetic ketoacidosis, metabolic acidosis, or renal failure. Table I lists the descriptions and causes of the various human respiratory patterns.

As described earlier, one of the key symptoms of the novel coronavirus is irregular or abnormal respiratory caused by the virus attack on lungs. It is of utmost significance to detect and identify the abnormal respiratory at the earliest stages in order to safeguard human lives. This paper focuses on the detec-

Umer Saeed and Syed Aziz Shah are with the Research Centre for Intelligent Healthcare, Coventry University, Coventry, UK (e-mail: saeedu3@uni.coventry.ac.uk; syed.shah@coventry.ac.uk).

Syed Yaseen Shah is with the School of Computing, Engineering and Built Environment, Glasgow Caledonian University, Glasgow, UK (e-mail: syedyaseen.shah@gcu.ac.uk).

Adnan Zahid is with the School of Engineering Physical Sciences, Heriot-Watt University, UK (e-mail: A.Zahid@hw.ac.uk).

Jawad Ahmad is with the School of Computing, Edinburgh Napier University, UK (e-mail: J.Ahmad@napier.ac.uk).

Muhammad Ali Imran and Qammer H. Abbasi are with the James Watt School of Engineering, University of Glasgow, Glasgow, UK (e-mail: muhammad.imran@glasgow.ac.uk; qammer.abbasi@glasgow.ac.uk).

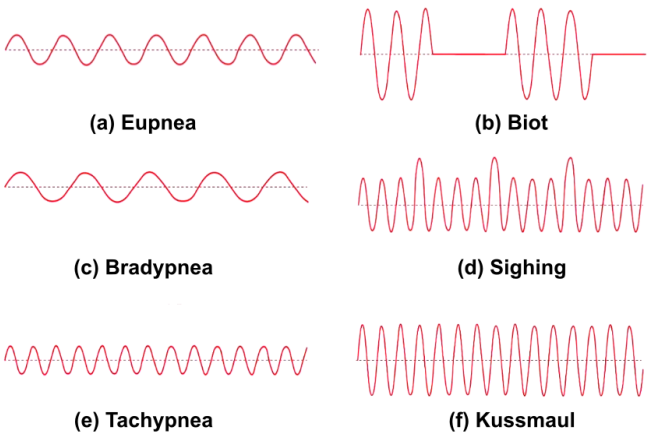

Fig. 1: Sample plots of distinct human respiratory.

TABLE I: Definition and distinct causes of human respiratory

Respiratory Type	Definition	Distinct Causes
Eupnea	Normal and healthy respiratory	Nutritious diet Healthy living
Biot	Intense respiratory with progressive breathless intervals	Concussion Spinal meningitis
Bradypnea	Sluggish and shallow respiratory	Concussion Sleeping Drugs Stroke Metabolic disorder
Sighing	Respiratory punctuated by repeated intense breathe	Dyspnea Giddiness Anxiety
Tachypnea	Rapid and shallow respiratory	Anxiety Fever Shock Workout
Kussmaul	Rapid and intense respiratory	Diabetic ketoacidosis Metabolic acidosis Renal failure

tion and diagnosis of abnormal human respiratory owing on COVID-19 through reliable non-contact wireless techniques merged with intelligent artificial intelligence algorithms. The advancement of universal, contactless, and wireless sensor technology to track everyday activities is gaining popularity everyday. Recently, various methods for monitoring human health and vital signs such as heart rate, have been established. Smart watches, portable sensors, Doppler RADAR, ultra-wideband RADAR, and frequency modulated carriers are some of the examples of it.

The rest of this paper is structured as follows: Section II provides a recent literature review towards non-invasive technology. In Section III, the details regarding proposed platform is provided. Section IV presents the experimental results and finally, Section V provides concluding remarks along with future research studies.

II. Literature Review

In this section, we have discussed distinct literature about non-invasive or non-contact sensing technologies and how they were utilised to detect and monitor various human activities and health conditions including symptoms of COVID-19 such as abnormal respiratory and heart rate.

A. Activity Monitoring using Non-invasive Technology

Authors in [3] utilised an ambient RADAR sensor to recognise various human activities in interior spaces and this system was able to classify a wide range of human activities. In [4], authors acquired RADAR spectrogram data to distinguish and categorise different types of falls in elderly humans. In [5], for fifteen distinct operations in the kitchen environment, a low powered RADAR sensor was employed. Authors in [6] developed a non-invasive passive detection system on a dynamic speed platform to recognise diverse human activities using commercial Wi-Fi. In [7]–[10], authors built a "Through the Wall" presence detection device for people that uses Wi-Fi signals to extract channel frequency response. A Wi-Fi-based gesture recognition system was designed that analyses fluctuations in Channel State Information (CSI) of Wi-Fi signals to monitor and identify distinct hand movements [11].

In [12], authors presented a methodology for identifying various eating activities utilising Wi-Fi signals, while the authors [13] developed a system for user identification for mobile devices utilising Wi-Fi technology. Using RF-based sensing, authors in [14] constructed a sleep guardian platform by integrating signal processing, machine learning, and edge computing. In [15], a Wi-Fi run system is built in the activity area for step estimation utilising CSI dynamics, whereas a Software Defined Radio (SDR) based non-contact system was created in [16] to recognise various human actions like standing, running, crawling, and so forth. Moreover, the authors in [17] generated a scheme based on SDR technology to hear various types of human speech, whilst [18] employed SDR technique to implement a whole house gesture recognition system.

B. Health Monitoring using Non-invasive Technology

Authors in [19] employed the passive doppler RADAR device to detect and classify distinct human respiration. Similarly in [20], human respiratory detection scheme was designed using a passive Doppler RADAR platform. In [21], Wi-Fi signals are used to monitor vital signs and recognise distinct body positions while sleeping. Authors in [22] and [23] employed the C-Band sensing techniques for various health monitoring concerns such as respiratory detection, tremor, and chronic obstructive pulmonary disease warning, whereas in [24] Res-Beat scheme was developed to track the rate of respiration.

In [25]–[27], authors developed a system based on S-band sensing techniques for a variety of health monitoring concerns, including seizure episode identification, cerebellar dysfunction patients' mobility evaluation, and pill rolling evaluation. Authors in [28] exploited the SDR-based technology to categorise various human exercising activities. Recently, in several literature, various machine/deep learning algorithms have been effectively applied to predict and diagnose COVID-19 symptoms using "Radio-graphic Imaging" [29]–[33].

III. Proposed Scheme

A. System Model

The scheme designed for this research work is made up of desktops that are utilised to run the SDR software in Laboratory Virtual Instrument Workbench (LabVIEW). The Universal Software Radio Peripheral (USRP) model "2922" is employed for SDR technology's general Radio-Frequency (RF) capabilities and omni-directional antennas for CSI capture. By observing small-scale motions in the wireless channel and obtaining fine-grained CSI, our system is able to recognise and categorise distinct respiratory patterns. The transmitter's RF signal travels via many multipaths to reach the receiver in an interior environment. This signal comprises data on environmental variables. The environment here is defined as the physical space that contains human aspects such as human postures, respiratory patterns, as well as environmental characteristics [35].

When a human is present in physical space, the reflection or diffraction of signals from its body creates a supplementary channel. As a result, the influence of human movement (either small or big) is recorded on the signal propagation and reported in the form of CSI on the received signals. Subsequently, the data from CSI can be utilised to identify distinct respiratory patterns. The USRP transmitter continually emits wireless signals with a certain frequency and the USRP receiver, on the other hand, receives these transmitted signals. Meanwhile, respiratory activity causes a minute deviation in the chest and abdomen, resulting in a shift in the signal propagation route recorded by the received signals in the CSI form. As illustrated in Figure 2, this non-invasive SDR-based scheme consists of three key functional blocks: the transmitter, radio or wireless channel, and receiver.

1) Transmitter: The transmitter is made up of two parts: the desktop and the USRP device. Pseudo random data bits are generated in the transmitter and transferred to quadrature amplitude modulation symbols or signs. These signs are then separated into two streams. In each parallel framework, reference data signs are concatenated. These reference signs are useful for the channel estimate on the receiver side. Every framework has zeros at the borders and one zero at DC. The Inverse Fast Fourier Transform (IFFT) function is used to convert frequency-domain signals into time-domain signals after zero padding. Each framework at the starting has a Cyclic Prefix (CP), which is created by replicating the last one-fourth point. This addition of CP will aid in the elimination of frequency and time offset at the receiver side. The synthesised data from the host desktop is transferred to the USRP device at a rate of "20 MS/s" over gigabit ethernet. The USRP uses a Digital Up Conversion (DUC) to convert the incoming signal to "400 MS/s", and then uses a digital-to-analog converter to transform the signals into analogue. The resulting analogue signal is blended up to the specified carrier frequency after passing through a low pass filter with a "20 MHz" bandwidth. This signal is then sent to an amplifier transmit, where the strength can be assorted from 0 to 30 dB. The signal is then broadcasted using an omni-directional antenna.

TABLE II: Human subjects information who participated in experiment

No.	Gender	Age	Weight (Kg)	Height (cm)	Physique Type
1	Male	28	65	179	Ectomorph
2	Male	26	76	173	Endomorph
3	Male	31	52	176	Endomorph
4	Male	31	65	174	Endomorph
5	Male	31	52	177	Ectomorph

2) Radio Channel: In this part of the scheme, an indoor radio channel is employed to gather information on distinct respiratory patterns due to minute human motions while breathing. The multi-path signals created by human body motions in between the two omni-direction antennas comprise the CSI signal.

3) Receiver: The signal is initially obtained by the USRP equipment through the omni-directional antenna on the receiving side. After passing this signal via a Low Noise Amplifier (LNA) to minimise the noise factor, it is then routed via a Drive Amplifier (DA) to alter the gain. The resulting signal is blended into a base-band complex signal utilising the Direct Conversion Receiver (DCR). The signal is then sampled at "100 MS/s" by a two channel analog-to-digital converter after passing through a Low Pass Filter (LPF) with a "20 MHz" bandwidth. This digitised complex signal is subsequently sent to a Digital Down Converter (DDC), which mixes, filters, and decimates it to a user-specified rate. Finally, at up to "20 MS/s", this down-converted signal is delivered to the host desktop via gigabit ethernet connection. The receiver host desktop not only eliminates CP from each framework, but also utilises the "Van de Beek" algorithm to eliminate frequency and time offset. The Fast Fourier Transform (FFT) is used to transform the time domain Orthogonal Frequency-Division Multiplexing (OFDM) instances into frequency domain OFDM instances once the CP is removed from each framework. The frequency domain signal's amplitude response is then extracted to determine distinct patterns of respiration.

B. Diagnosis Approach

The primary steps involved in the abnormal respiratory diagnosis approach are shown in Figure 3 and are explained as follows.

1) Data Acquisition: The data on respiration were collected in a laboratory setting, which illustration is presented in Figure 3. The experimental setup consists of two USRP (NI-2922), with a spacing of one metre between the USRP device and the human participant. Each participant was instructed to sit in a relaxed position with the least body movements. Both USRP devices are parallel to the participant's abdomen and situated at the same height. Table II lists the details of each of the five individuals who were instructed to practise different respiratory patterns.

Participant were instructed to do each respiratory pattern appropriately as per medical instructions before respiratory information was acquired. Each human subject in this study was instructed to perform six different respiratory: eupnea, biot, bradypnea, sighing, tachypnea, and kussmaul. A total

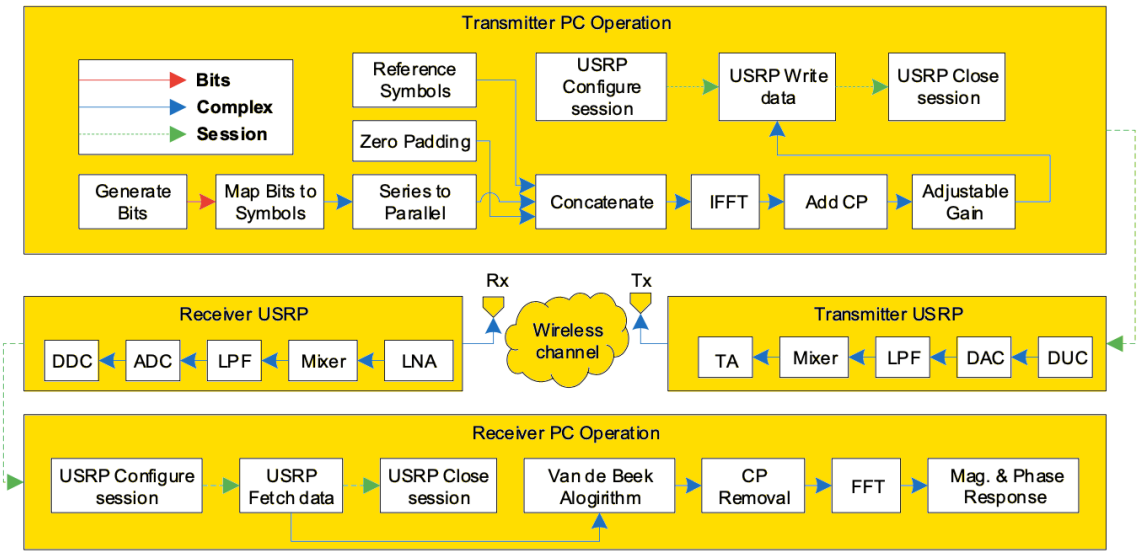

Fig. 2: Illustration of proposed SDR-based non-invasive scheme for abnormal respiratory diagnosis [34].

of 150 experiments are conducted for six distinct respiratory patterns and lastly, six datasets are obtained from five human participants. Participants performed each respiratory activity for thirty seconds. To assure and obtain a greater degree of precision, comprehensive experiments are carried out.

2) Data Wrangling: After data acquisition, the data were processed in order to eliminate unwanted noise and extract important respiratory features. The obtained OFDM signal is exploited for fine-grained CSI extraction at the receiver end. The amplitude and phase frequency responses from the obtained OFDM signal can be acquired. However, only the amplitude frequency response is employed for further processing in this study. The respiratory activity is identified by following the acquisition of the amplitude frequency response for each respiratory activity. If the amplitude response closely resembles the real respiratory rate, it is approved; otherwise, it is rejected, and the individual is requested to repeat the respiratory pattern more effectively. The number of subcarriers, as well as the number of OFDM samples, are displayed in this amplitude response. The number of OFDM samples received is determined by a variety of parameters, including the amount of time it takes to complete each respiratory activity.

a) Subcarrier Selection: For each respiratory activity, the receiver acquires a set of 256 subcarriers. It is noted that the amplitude of every subcarrier reveals distinct sensitivity to respiratory patterns. To improve respiratory activity recognition, any subcarriers that are less sensitive to respiratory activity have to be removed. The variance of subcarriers is determined, and on this basis, all subcarriers with lower sensitivity to respiratory activity are eliminated, as shown in the data wrangling block of Figure 3.

b) Outliers Removal: Wavelet filtering is applied after subcarrier selection. As illustrated in the second block of the data wrangling process in Figure 3, the wavelet filter not only eliminates outliers from the raw data but also preserves crisp transitions. Soft heuristic threshold is used for wavelet filtering with scaled noise parameters with detail coefficients at level 4 using wavelet Symlets-5 (sym5).

c) Refined Data: A moving average filter with window size 8 is employed to refine the data further and eliminate high frequency noise not caused by respiratory activity, as depicted in Figure 3. Various respiratory patterns can easily be identified after conducting the afore-mentioned data wrangling processes.

3) Deep Multilayer Perceptron Classifier: After distinct layers of data processing and respiratory features extraction, at last the data were trained by Deep Multilayer Perceptron (DMLP) classifier. The DMLP is a supervised deep learning technique where a feedforward artificial neural network produces a number of outputs from a set of inputs. Several layers of input neurons are linked as a directed graph between both the input and output layers of the DMLP. Backpropagation technique is utilised by DMLP classifier in order to train the network. Substantially, a neural network linking several layers of a directed graph is a multilayer perceptron, meaning that the signal flows one way across the neurons. Each neuron has a nonlinear activation function besides the input neurons. The DMLP is commonly used to address problems that need supervised learning approach such as speech recognition, machine translation, image recognition, and anomaly detection [36]–[41].

IV. Simulation Results and Analysis

A. Respiratory Data

This section provides a detailed description about each respiratory pattern utilising SDR-based RF sensing. Five separate participants conducted each respiratory activity and each individual knew the features of all breath patterns through sufficient instructions and training before doing these diverse respiratory tasks. For a few times, each participant has been instructed to practise these patterns of respiratory and the outcomes for six distinct respiratory patterns are then achieved. In order to evaluate these respiratory patterns, the CSI amplitude response is utilised. Figure 4 displays the findings

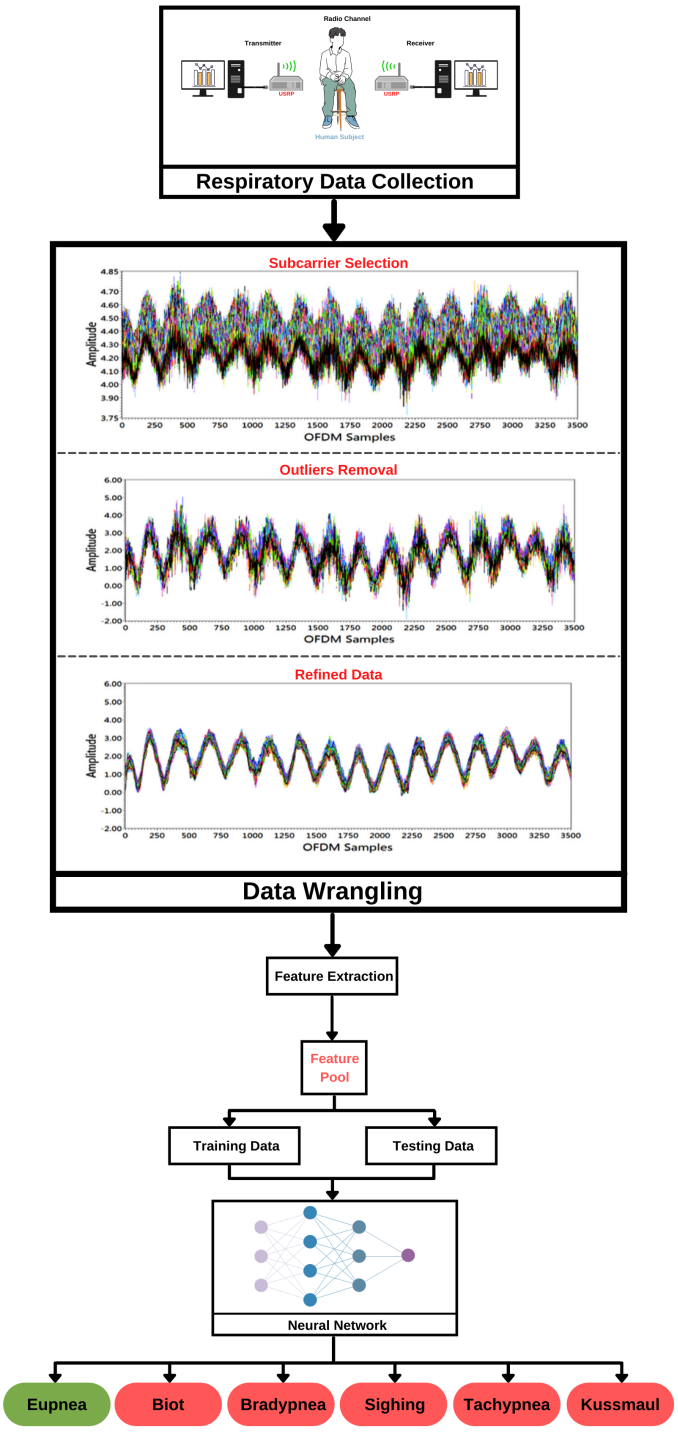

Fig. 3: Framework of the applied model for abnormal respiratory diagnosis.

for six distinct respiratory activities and the amplitude of respiratory patterns in all subcarriers. Due to every activity across 3500 OFDM samples, changes in amplitude reaction are achieved. The outcome of each type of respiratory is discussed as follows.

a) Eupnea: Eupnea is a normal pace of respiratory and adults normally have 12-20 breaths per minute in the case of eupnea. The participants were asked to breathe properly and at a regular pace in order to obtain eupnea respiratory pattern. Figure 4(a) shows that there are 10 breaths each half-minute, which corresponds to the respiratory patterns depicted in Figure 1(a).

b) Biot: Biot is a deep respiratory practice that alternates with intervals of no respiration. The participants were asked to practise and perform this respiratory pattern and Figure 4(b) shows that deep respiratory were followed by breathless intervals, which corresponds to the respiratory patterns depicted in Figure 1(b).

c) Bradypnea: The bradypnea is a type of respiratory that is sluggish and shallow. The participants were asked to breathe more slowly than usual in order to acquire this respiratory. Figure 4(c) shows that six breaths were taken every thirty seconds, which corresponds to the respiratory patterns depicted in Figure 1(c).

d) Sighing: Sighing is a type of respiratory pattern that includes numerous intense breaths. To acquire a sighing respiratory, the normal respiratory was disrupted by many intense breaths, as indicated in Figure 4(d), which corresponds to the respiratory patterns depicted in Figure 1(d).

e) Tachypnea: Tachypnea is characterised by rapid and shallow respiration process. The participants were instructed to breathe quicker than typical in order to obtain this respiratory pattern. Figure 4(e) shows that thirteen breaths were taken every thirty seconds, which corresponds to the respiratory patterns depicted in Figure 1(e).

f) Kussmaul: The kussmaul is a respiratory that is both quick and deep. The rapid and intense breaths can be noted in Figure 4(f), which corresponds to the respiratory patterns depicted in Figure 1(f).

B. Results

We have recruited healthy participants with various age range and ask them to mimic the particular six breathing pattern, which were efficiently detected by the proposed model. Each respiratory dataset consisted of 3650×3500 observations or data points. Considering the six above-mentioned respiratory classes, the final dataset were composed of $6 \times 3650 \times 3500$ data points. In each respiratory class, 50% of the data samples were used to train the machine learning classifier, whereas 25% of the data samples were used for validation purposes and remaining 25% for testing. In this work, a multi-class classification technique was adopted to classify (or diagnose) each respiratory and the data samples were labelled accordingly.

To execute the simulations, the DMLP algorithm used in this study was programmed in Python. The "Grid Search Cross-Validation" methodology was adopted for the validation part of the dataset in order to optimize the hyperparameters for DMLP. This methodology uses the principles of fit and score to discover the appropriate parameters for training machine learning models. These parameters are provided in Table III. Moreover, using a single performance assessment metric for machine learning models is often not regarded as best practise. Hence, to evaluate the performance of the algorithms, five different metrics were used: confusion matrix, precision,

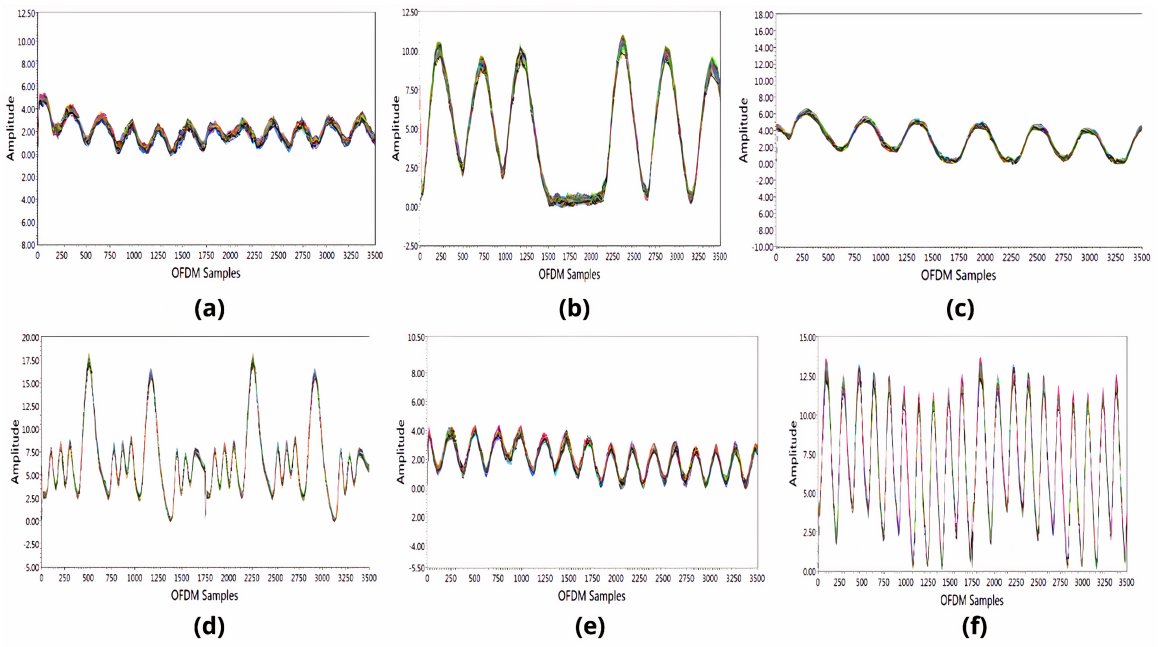

Fig. 4: Extracted patterns of distinct human respiratory: (a) Eupnea (b) Biot (c) Bradypnea (d) Sighing (e) Tachypnea (f) Kussmaul [42].

TABLE III: Parameters obtained by the cross-validation technique for training the DMLP classifier

Algorithm	Hyperparameters
Deep Multilayer Perceptron	hidden layer sizes = 100 max iteration = 400 solver = lbfgs activation = identity learning rate = constant

recall, f1-score/f-measure, and diagnosis accuracy [43] (see Equation 1, 2, 3, 4).

$$\frac{Diagnosis}{Accuracy} = \frac{Number\ of\ respiratory\ diagnosed}{Total\ number\ of\ respiratory} \quad (1)$$

$$F1 - score = 2 \times \left(\frac{Recall \times Precision}{Recall + Precision}\right) \quad (2)$$

$$Precision = \frac{True\ Positives}{Predicted\ Positives} \quad (3)$$

$$Recall = \frac{True\ Positives}{Actual\ Positives} \quad (4)$$

In this work, we exploited two distinct machine learning classifiers: Deep Multilayer Perceptron (DMLP) and Random Forest (RF). The reason to choose two various classifiers is to evaluate the performance on different respiratory. Although DMLP achieved a slightly higher accuracy than RF, nevertheless both classifiers almost performed the same. Table IV shows the overall accuracy accomplished by the DMLP and the RF.

Moreover, Figure 5 exhibits the confusion matrix for diverse respiratory classifications. As can be seen in Figure 5(a), DMLP has only 12 misclassifications of eupnea with biot

TABLE IV: Overall accuracy achieved by the DMLP and the RF classifier for six various respiratory classes

Classifier	Overall Accuracy
Deep Multilayer Perceptron	99%
Random Forest	98%

respiratory class, whereas the biot class has merely 19 misclassified points with eupnea and 5 with bradypnea. This is due to the fact that these classes have highly similar structure than other classes. Rest of the classes such as bradypnea, sighing, tachypnea, and kussmaul have either 1 or 2 misclassified points, therefore resulting in accuracy up to 99%. Furthermore, Figure 5(b) demonstrates the performance of RF classifier. As can be noted, RF has slightly higher misclassified points than DMLP, nevertheless, RF resulted in accuracy up to 98%.

In Figure 6, the performance of DMLP and RF in terms of precision, recall, and f1-score is revealed on six different respiratory classes: eupnea, biot, bradypnea, sighing, tachypnea, and kussmaul. As shown in Figure 6(a), DMLP attained 98% precision for eupnea, 99% for biot and bradypnea, 100% for sighing, tachypnea, and kussmaul. In terms of recall, DMLP attained 99% for eupnea, 97% for biot, and 100% for bradypnea, sighing, tachypnea, and kussmaul. In the case of f1-score, DMLP attained 98% for eupnea and biot, whereas 100% for bradypnea, sighing, tachypnea, and kussmaul. Furthermore, in Figure 6(b), performance of RF classifier can be noted. In the context of precision, RF obtained 95% performance for eupnea, 97% for biot, 98% for bradypnea, 100% for sighing and kussmaul, and 99% for tachypnea. In terms of recall, RF obtained 97% for eupnea and biot, 98% for bradypnea, 99% for sighing and kussmaul, and 100% for tachypnea. In the case of f1-score, RF obtained 96% performance for eupnea, 97%

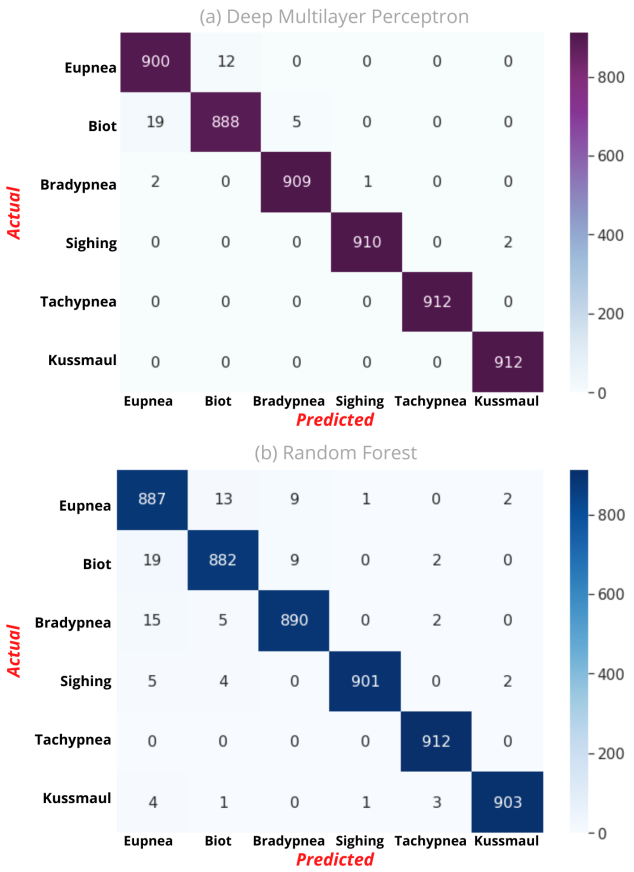

Fig. 5: Confusion matrix of six distinct respiratory classification: (a) Deep Multilayer Perceptron and (b) Random Forest.

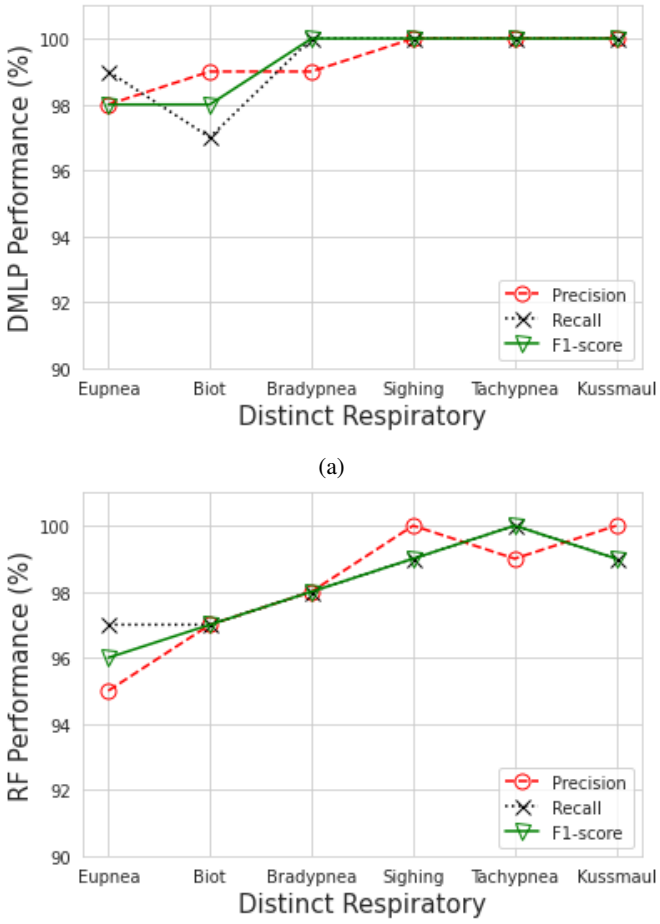

Fig. 6: Precision, recall, and f1-score comparison for individual respiratory class on: (a) Deep Multilayer Perceptron Classifier and (b) Random Forest Classifier.

for biot, 98% for bradypnea, 99% for sighing and kussmaul, whereas 100% for tachypnea.

C. Future Work

There are certain limitations associated with this study, which we aim to overcome in the future research work. We would consider more realistic environment and conduct experiments in noisy environment and in different body postures. Furthermore, the proposed scheme can be utilised for a single subject at a time in a static and controlled environment. Apart from that, the experiments were not conducted on real COVID-19 infected patients due to several concerns. As a result, the future recommendations would be to add respiratory patterns of several subjects in a non-static environment, employing more advanced algorithms and utilising the SDR-based platform's versatility. Moreover, real-time data acquisition of COVID-19 infected patients shall be carried out in order to construct a more realistic model. Other than that, more respiratory patterns such as ataxic and cheynestokes shall be explored in order to enhance the system's reliability.

V. Conclusion

While in the midst of the COVID-pandemic, non-invasive strategies help minimise the burden on healthcare professionals, as well as require the least amount of involvement from affected individuals. Studies on recently diagnosed patients show that a COVID-19 infection affects respiratory or breathing patterns differently in comparison to flu or a cold. In some cases, COVID-19 infection is marked by an accelerated respiratory rate and that calls for constant monitoring of respiratory patterns. In this paper, a non-invasive or contactless SDR-based platform merged with intelligent machine learning algorithms is proposed. The system is designed for the detection and monitoring of primarily six distinct human respiratory patterns including normal and abnormal such as eupnea, biot, bradypnea, sighing, tachypnea, and kussmaul. The respiratory data employed for this study were acquired from five different subjects. Using fine-grained OFDM signals, the fluctuations in CSI caused by human respiration were used to detect distinct respiratory patterns. Then, using the Deep Multilayer Perceptron classifier, these respiratory patterns were effectively classified attaining accuracy of up to 99%. As a result, it can be stated that SDR-based Radio-Frequency sensing is a viable approach in an indoor setting for detecting and classifying several respiratory patterns linked to various illnesses, whether COVID-19 infection or any other disease.

REFERENCES

[1] P. K. Ozili and T. Arun, "Spillover of covid-19: impact on the global economy," *Available at SSRN 3562570*, 2020.

[2] W. Ganong, "Review of medical physiology: Norwalk," *Appleton and Lang*, pp. 438–465, 1993.

[3] S. Zhu, J. Xu, H. Guo, Q. Liu, S. Wu, and H. Wang, "Indoor human activity recognition based on ambient radar with signal processing and machine learning," in *2018 IEEE international conference on communications (ICC)*. IEEE, 2018, pp. 1–6.

[4] W. Taylor, K. Dashtipour, S. A. Shah, M. A. Imran, and Q. H. Abbasi, "Image classification of radar spectograms of human motion using machine and deep learning algorithms," *IEEE Sensors Journal*, 2020.

[5] F. Luo, S. Poslad, and E. Bodanese, "Kitchen activity detection for healthcare using a low-power radar-enabled sensor network," in *ICC 2019-2019 IEEE International Conference on Communications (ICC)*. IEEE, 2019, pp. 1–7.

[6] K. Qian, C. Wu, Z. Yang, Y. Liu, F. He, and T. Xing, "Enabling contactless detection of moving humans with dynamic speeds using csi," *ACM Transactions on Embedded Computing Systems (TECS)*, vol. 17, no. 2, pp. 1–18, 2018.

[7] S. Di Domenico, M. De Sanctis, E. Cianca, and M. Ruggieri, "Wifi-based through-the-wall presence detection of stationary and moving humans analyzing the doppler spectrum," *IEEE Aerospace and Electronic Systems Magazine*, vol. 33, no. 5-6, pp. 14–19, 2018.

[8] X. Yang, S. A. Shah, A. Ren, D. Fan, N. Zhao, S. Zheng, W. Zhao, W. Wang, P. J. Soh, and Q. H. Abbasi, "S -band sensing-based motion assessment framework for cerebellar dysfunction patients," *IEEE Sensors Journal*, vol. 19, no. 19, pp. 8460–8467, 2019.

[9] S. A. K. Tanoli, M. Rehman, M. B. Khan, I. Jadoon, F. Ali Khan, F. Nawaz, S. A. Shah, X. Yang, and A. A. Nasir, "An experimental channel capacity analysis of cooperative networks using universal software radio peripheral (usrp)," *Sustainability*, vol. 10, no. 6, p. 1983, 2018.

[10] D. Haider, A. Ren, D. Fan, N. Zhao, X. Yang, S. A. Shah, F. Hu, and Q. H. Abbasi, "An efficient monitoring of eclamptic seizures in wireless sensors networks," *Computers & Electrical Engineering*, vol. 75, pp. 16–30, 2019.

[11] M. A. A. Al-qaness and F. Li, "Wiger: Wifi-based gesture recognition system," *ISPRS International Journal of Geo-Information*, vol. 5, no. 6, p. 92, 2016.

[12] C. Wang, Z. Lin, Y. Xie, X. Guo, Y. Ren, and Y. Chen, "Wieat: Fine-grained device-free eating monitoring leveraging wi-fi signals," *arXiv preprint arXiv:2003.09096*, 2020.

[13] L. Cheng and J. Wang, "Walls have no ears: A non-intrusive wifi-based user identification system for mobile devices," *IEEE/ACM Transactions on Networking*, vol. 27, no. 1, pp. 245–257, 2019.

[14] Y. Gu, Y. Wang, Z. Liu, J. Liu, and J. Li, "Sleepguardian: an rf-based healthcare system guarding your sleep from afar," *IEEE Network*, vol. 34, no. 2, pp. 164–171, 2020.

[15] M. Liu, L. Zhang, P. Yang, L. Lu, and L. Gong, "Wi-run: Device-free step estimation system with commodity wi-fi," *Journal of Network and Computer Applications*, vol. 143, pp. 77–88, 2019.

[16] S. Savazzi, S. Sigg, M. Nicoli, V. Rampa, S. Kianoush, and U. Spagnolini, "Device-free radio vision for assisted living: Leveraging wireless channel quality information for human sensing," *IEEE Signal Processing Magazine*, vol. 33, no. 2, pp. 45–58, 2016.

[17] G. Wang, Y. Zou, Z. Zhou, K. Wu, and L. M. Ni, "We can hear you with wi-fi!" *IEEE Transactions on Mobile Computing*, vol. 15, no. 11, pp. 2907–2920, 2016.

[18] Q. Pu, S. Gupta, S. Gollakota, and S. Patel, "Whole-home gesture recognition using wireless signals," in *Proceedings of the 19th annual international conference on Mobile computing & networking*, 2013, pp. 27–38.

[19] W. Li, B. Tan, and R. Piechocki, "Passive radar for opportunistic monitoring in e-health applications," *IEEE journal of translational engineering in health and medicine*, vol. 6, pp. 1–10, 2018.

[20] W. Li, B. Tan, and R. J. Piechocki, "Non-contact breathing detection using passive radar," in *2016 IEEE International Conference on Communications (ICC)*. IEEE, 2016, pp. 1–6.

[21] J. Liu, Y. Chen, Y. Wang, X. Chen, J. Cheng, and J. Yang, "Monitoring vital signs and postures during sleep using wifi signals," *IEEE Internet of Things Journal*, vol. 5, no. 3, pp. 2071–2084, 2018.

[22] Q. Zhang, D. Haider, W. Wang, S. A. Shah, X. Yang, and Q. H. Abbasi, "Chronic obstructive pulmonary disease warning in the approximate ward environment," *Applied Sciences*, vol. 8, no. 10, p. 1915, 2018.

[23] D. Haider, A. Ren, D. Fan, N. Zhao, X. Yang, S. A. K. Tanoli, Z. Zhang, F. Hu, S. A. Shah, and Q. H. Abbasi, "Utilizing a 5g spectrum for health care to detect the tremors and breathing activity for multiple sclerosis," *Transactions on Emerging Telecommunications Technologies*, vol. 29, no. 10, p. e3454, 2018.

[24] X. Wang, C. Yang, and S. Mao, "Resilient respiration rate monitoring with realtime bimodal csi data," *IEEE Sensors Journal*, vol. 20, no. 17, pp. 10 187–10 198, 2020.

[25] S. A. Shah, D. Fan, A. Ren, N. Zhao, X. Yang, and S. A. K. Tanoli, "Seizure episodes detection via smart medical sensing system," *Journal of Ambient Intelligence and Humanized Computing*, pp. 1–13, 2018.

[26] X. Yang, S. A. Shah, A. Ren, D. Fan, N. Zhao, S. Zheng, W. Zhao, W. Wang, P. J. Soh, and Q. H. Abbasi, "*s*-band sensing-based motion assessment framework for cerebellar dysfunction patients," *IEEE Sensors Journal*, vol. 19, no. 19, pp. 8460–8467, 2018.

[27] S. A. Shah, X. Yang, and Q. H. Abbasi, "Cognitive health care system and its application in pill-rolling assessment," *International Journal of Numerical Modelling: Electronic Networks, Devices and Fields*, vol. 32, no. 6, p. e2632, 2019.

[28] M. A. M. Al-hababi, M. B. Khan, F. Al-Turjman, N. Zhao, and X. Yang, "Non-contact sensing testbed for post-surgery monitoring by exploiting artificial-intelligence," *Applied Sciences*, vol. 10, no. 14, p. 4886, 2020.

[29] W. Shi, L. Tong, Y. Zhu, and M. D. Wang, "Covid-19 automatic diagnosis with radiographic imaging: Explainable attentiontransfer deep neural networks," *IEEE Journal of Biomedical and Health Informatics*, 2021.

[30] C. C. John, V. Ponnusamy, S. K. Chandrasekaran, and R. Nandakumar, "A survey on mathematical, machine learning and deep learning models for covid-19 transmission and diagnosis," *IEEE reviews in biomedical engineering*, 2021.

[31] S. Tabik, A. Gómez-Ríos, J. L. Martín-Rodríguez, I. Sevillano-García, M. Rey-Area, D. Charte, E. Guirado, J. L. Suárez, J. Luengo, M. Valero-González *et al.*, "Covidgr dataset and covid-sdnet methodology for predicting covid-19 based on chest x-ray images," *IEEE journal of biomedical and health informatics*, vol. 24, no. 12, pp. 3595–3605, 2020.

[32] Y. Jiang, H. Chen, M. Loew, and H. Ko, "Covid-19 ct image synthesis with a conditional generative adversarial network," *IEEE Journal of Biomedical and Health Informatics*, 2020.

[33] F. Shi, J. Wang, J. Shi, Z. Wu, Q. Wang, Z. Tang, K. He, Y. Shi, and D. Shen, "Review of artificial intelligence techniques in imaging data acquisition, segmentation and diagnosis for covid-19," *IEEE reviews in biomedical engineering*, 2020.

[34] M. Rehman, R. A. Shah, M. B. Khan, N. A. A. Ali, A. A. Alotaibi, T. Althobaiti, N. Ramzan, S. A. Shaha, X. Yang, A. Alomainy *et al.*, "Contactless small-scale movement monitoring system using software defined radio for early diagnosis of covid-19," *IEEE Sensors Journal*, 2021.

[35] Z. Yang, Z. Zhou, and Y. Liu, "From rssi to csi: Indoor localization via channel response," *ACM Computing Surveys (CSUR)*, vol. 46, no. 2, pp. 1–32, 2013.

[36] X. Yang, D. Fan, A. Ren, N. Zhao, and M. Alam, "5g-based user-centric sensing at c-band," *IEEE Transactions on Industrial Informatics*, vol. 15, no. 5, pp. 3040–3047, 2019.

[37] S. U. Jan, Y.-D. Lee, J. Shin, and I. Koo, "Sensor fault classification based on support vector machine and statistical time-domain features," *IEEE Access*, vol. 5, pp. 8682–8690, 2017.

[38] X. Yang, L. Guan, Y. Li, W. Wang, Q. Zhang, M. U. Rehman, and Q. H. Abbasi, "Contactless finger tapping detection at c-band," *IEEE Sensors Journal*, vol. 21, no. 4, pp. 5249–5258, 2020.

[39] U. Saeed, S. U. Jan, Y.-D. Lee, and I. Koo, "Fault diagnosis based on extremely randomized trees in wireless sensor networks," *Reliability Engineering & System Safety*, vol. 205, p. 107284, 2021.

[40] X. Yang, S. A. Shah, A. Ren, N. Zhao, Z. Zhang, D. Fan, J. Zhao, W. Wang, and M. Ur-Rehman, "Freezing of gait detection considering leaky wave cable," *IEEE Transactions on Antennas and Propagation*, vol. 67, no. 1, pp. 554–561, 2018.

[41] Z. Ahmad, A. Rai, A. S. Maliuk, and J.-M. Kim, "Discriminant feature extraction for centrifugal pump fault diagnosis," *IEEE Access*, vol. 8, pp. 165 512–165 528, 2020.

[42] M. Rehman, R. A. Shah, M. B. Khan, N. A. AbuAli, S. A. Shah, X.-D. Yang, A. Alomainy, M. A. Imran, and Q. H. Abbasi, "Rf sensing based breathing patterns detection leveraging usrp devices," *Sensors*, pp. In–Press, 2021.

[43] C. Goutte and E. Gaussier, "A probabilistic interpretation of precision, recall and f-score, with implication for evaluation," in *European conference on information retrieval*. Springer, 2005, pp. 345–359.